

Acoustic resonance of an air-filled Elasto-bubble

F. Delmotte,¹ V. Leroy,¹ and J. Zhang^{1,2}

¹Université Paris Cité, CNRS, Laboratoire Matière et Systèmes Complexes UMR 7057, 75231 Paris cedex 13, France

²PMMH, CNRS, ESPCI Paris, Université PSL, Sorbonne Université, Université de Paris, F-75005, Paris, France.

(*Electronic mail: jishen.zhang@espci.fr.)

(Dated: 7 April 2026)

We propose the use of an *in-house* air-filled elasto-bubble as a novel subwavelength acoustic resonator. Building on the well-established physics of gas bubbles, and incorporating an elastic shell, we experimentally demonstrate that these elasto-bubbles retain the key acoustic properties of classical bubbles. Indeed, through experiments performed in an impedance tube, we observe a strong acoustic response and efficient transmission reduction, in good agreement with the theory considering a layered bubble introduced by Alekseev and Rybak (1999)¹. Finally, elasto-bubbles offer a simple and effective route to tunable acoustic resonances through independent control of their radius and shell thickness.

Metamaterials are artificial structures that show unusual properties, such as negative refraction². They are often made by using sub-wavelength resonators, which fulfill the twofold condition of a strong interaction with the incoming wave (resonator) and the emergence of an effective medium (sub-wavelength). For electromagnetic waves, the idiomatic example is the split-ring resonator³. In acoustics,⁴ some examples include Helmholtz resonators⁵, membranes⁶ and bubbles⁷. The latter is particularly interesting for water borne acoustics, because its resonance is at deep sub-wavelength. A quantity to appreciate this fact is the product of the resonance frequency of the scatterer and its radius f_0R , to be compared to the wave velocity in the host medium. For a bubble in water that resonates at the Minnaert frequency⁸, $f_0R = 3.2$ m/s, compared to 1500 m/s, which gives a factor of almost 500 between the radius of the bubble and the wavelength. Applications for super-absorption of water-borne waves have been developed with bubbles in soft media, in the ultrasonic and audible frequency ranges. In this paper, we discuss the possibility of using bubbles for air-borne acoustics. Our idea is that the physical mechanism behind bubble resonance is that of a mass-spring harmonic oscillator, with stiffness determined by the compressibility of the gas and inertia determined by the displaced surrounding media. For water-borne acoustics, the inertia is large because there is water all around the bubble. For air-borne acoustics, we wanted to explore the possibility of an air-water-air system, i.e. a thin layer of water that would enclose a pocket of gas. For practical reasons, such as ease of handling and bubble stability, the layer of water is replaced by a layer made of a soft elastic material. The acoustic scattering of such an object can be easily determined by using the work by Alekseev and Rybak¹, who derived a general expression for the scattering function of a bubble with an elastic shell in an elastic medium. Let us consider a gas bubble of radius R , surrounded by a shell of thickness h made of a material with density ρ and shear modulus $\mu = \mu' + i\mu''$. The embedding medium is air with density and wavenumber noted ρ_a and k_a respectively. We will call this layered bubble an elasto-bubble. For an incoming plane wave $p \exp(ik_ax)$ propagating in the x direction with an amplitude p , it can be shown that, in the limit of a large wavelength compared to R , the elasto-bubble

scatters a radial spherical wave $f_{\text{scat}} p \exp(ik_ar)/r$, with a scattering function given by

$$f_{\text{scat}} = \frac{R^*}{(\omega_0/\omega)^2 - 1 - i(\delta + k_a R^*)}, \quad (1)$$

with, at first order in h/R

$$R^* = R \frac{\rho_a R + \rho_a h}{\rho_a R + \rho h}, \quad (2)$$

$$\omega_0^2 = \frac{3\kappa P_0 + 12\mu' h/R}{\rho_a R^3} R^*, \quad (3)$$

$$\delta = \frac{12\mu'' h/R}{\omega^2 \rho_a R^3} R^*, \quad (4)$$

where κ is the polytropic exponent for the gas. If the density contrast between the shell and the gas is higher than the radius to thickness ratio of the elasto-bubble ($\rho h / (\rho_a R) \gg 1$), the effective radius can be approximated by $R^* \simeq \rho_a R^2 / (\rho h)$. If furthermore, the shear modulus of the shell is low enough to ensure that $\mu' h/R \ll \kappa P_0/4$, the resonance frequency reduces to:

$$\omega_0^2 = \frac{3\kappa P_0}{\rho R h}. \quad (5)$$

It leads to a resonance frequency of the form $f_0 R = \sqrt{R/h} \times 3.2$ m/s. As expected, the resonance is not as low as in the case of a bubble in water, because of the limited amount of heavy material contributing to the inertia. Nevertheless, the system remains strongly subwavelength. For $R/h = 10$, we obtain $f_0 R \simeq 10$ m/s, corresponding to a wavelength in air about 34 times larger than the radius of the elasto-bubble. This highlights the ability of such objects to interact with acoustic waves much larger than their own size.

We fabricated elasto-bubble to test the validity of Eq. (5). For a soft elastomer with a density close to that of water, a resonance frequency of about 1 kHz is expected for $R = 20$ mm and $h = 0.5$ mm. To fabricate the elasto-bubbles in the targeted range of radii and shell thicknesses, we used an *in-house* viscous coating protocol⁹. A liquid polymer mixture was first deposited into each hemisphere of a spherical mold and spread

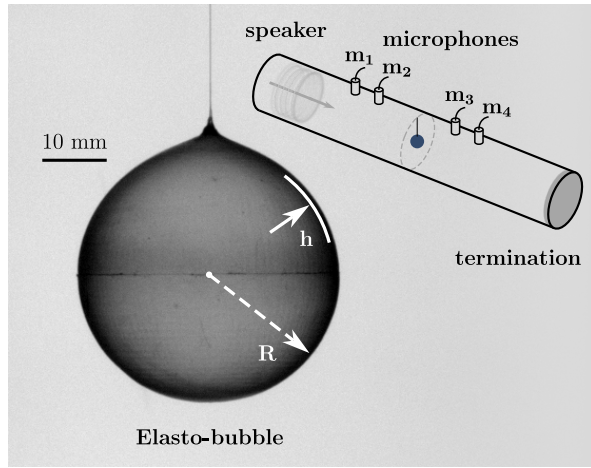


FIG. 1. Shape of an elasto-bubble suspended on a thin wire. The annotations indicate the radius R of the elasto-bubble and the shell thickness h . Inset: schematic of the experimental setup.

over the inner surface. The hemispheres were then placed bottom-down to allow excess liquid to drain. After draining, the mold was sealed and mounted on a planetary rotating platform during curing in order to smooth residual thickness heterogeneities. Once the elastomer was fully cross-linked, the intact shell was demolded, remaining filled with air without additional inflation, resulting in negligible in-plane tension of the shell. A highly compliant PDMS-based elastomer (Ecoflex 00-30) was used, with an elastic modulus $\mu' \approx 26$ kPa. The thickness of the shell was deduced from the weight of the elasto-bubble: $m = 4\pi\rho(R_{\text{ext}}^3 - (R_{\text{ext}} - h)^3)/3$, with $\rho = 1070 \text{ kg/m}^3$, the density of the elastomer. Five elasto-bubbles of varying radii and shell thicknesses were manufactured, as listed in Table I, in which we report the theoretical resonance frequency predicted by Eq. (5). Fig. 1 shows a picture of elasto-bubble No.2.

No.	R_{ext} (mm)	m (g)	h (μm)	f_0 (Hz)
1 ▽	21	1.94	332.4 ± 1.7	1211.0 ± 3.1
2 ○	21	2.53	435.6 ± 1.8	1060.4 ± 2.1
3 □	21	3.79	659.7 ± 1.8	866.5 ± 1.1
4 △	15	1.08	365.8 ± 3.5	1371.8 ± 6.3
5 ◇	10	0.64	500.6 ± 8.2	1455.5 ± 11.3

TABLE I. Parameters of the 5 elasto-bubbles fabricated and characterized in this study. R_{ext} is the radius of the mold used to fabricate the elasto-bubble. m is the mass of the elasto-bubble, from which the thickness h is deduced. From these geometrical parameters, theoretical resonance frequency f_0 is evaluated from Eq.(5).

The acoustic response of the elasto-bubbles is characterized using a commercial impedance tube (B&K 4206-T) capable of generating plane acoustic waves in the frequency range 0.3–5 kHz. The tube has a uniform inner radius $R_t=50$ mm (*cf* Fig. 1). A speaker is placed at one end of the tube, and four condenser microphones type 4187 (m1–m4) are positioned along the tube to measure the acoustic field. Two mi-

crophones (m1 and m2) are located upstream of the test section, while two others (m3 and m4) are placed downstream. The tube has a finite length, with multiple reflections. However, following a standard procedure¹⁰ that prescribes to measure the acoustic response of the system with two different terminations, one can determine \mathcal{T} and \mathcal{R} , the transmission and reflection coefficients of the sample placed in the middle of the tube. In our case, the sample was a elasto-bubble, suspended along the central axis of the tube between microphones m2 and m3 using a thin nylon wire of diameter 0.1 mm, minimizing its influence on the acoustic field. At rest, the elasto-bubble was free to deform under gravity and adopted a slightly asymmetric (pear-like) shape during the measurement (Fig. 1). A potential limitation of the experimental protocol is a gradual loss of gas from the elasto-bubble, which may originate either from permeation through the PDMS-based elastomer shell^{11,12} or from possible microscopic defects. Such a loss would lead to a decrease of the internal volume and, consequently, of the effective radius of the elasto-bubble, potentially affecting both the measured acoustic response and the comparison with model predictions. To evaluate potential variations of the elasto-bubble volume, independent imaging measurements are performed prior to and after the acoustic experiments. The elasto-bubble shape is extracted from images, allowing the volume to be estimated and an effective radius to be deduced. These measurements confirm that the elasto-bubble conserves its initial volume within experimental uncertainty over the duration of the experiments.

Fig. 2 a-b shows the transmission amplitude and the phase (respectively $|\mathcal{T}|$ and $\text{phase}(\mathcal{T})$) measured for elasto-bubble No.2 in the impedance tube. A sharp drop of transmission is observed at $f_{\text{min}} = 1.1$ kHz, accompanied by an accident in the phase, indicating a strong interaction between the acoustic wave and the elasto-bubble. Fig. 2 c shows the amount of energy absorbed by the elasto-bubble, called absorption and noted $\mathcal{A} = 1 - |\mathcal{R}|^2 - |\mathcal{T}|^2$, which reaches a maximum of 0.34 .

The accident in the transmission at a frequency close to the resonance frequency predicted by the model ($f_0 = 1.06$ kHz for this object, see Table I) is a first indication that the elasto-bubble behaves as expected. A more quantitative comparison was obtained by calculating the transmission and reflection coefficients predicted by the theory. For a monopole in a square duct, we can use image monopoles to satisfy the zero-displacement conditions on the walls of the duct. This is equivalent to considering an infinite plane of monopoles arranged on a square lattice. This configuration was shown to lead to^{14,15}

$$\mathcal{R} = \frac{iKf_{\text{scat}}}{1 - iKf_{\text{scat}}B} \quad (6)$$

$$\mathcal{T} = 1 + \mathcal{R} \quad (7)$$

where $K = 2/(k_a R_t^2)$ and $B = 1 + ik_a R_t - (k_a R_t)^2/2$. Here we make the assumption that the circular tube gives a response similar to the square duct of the same surface. Inject-

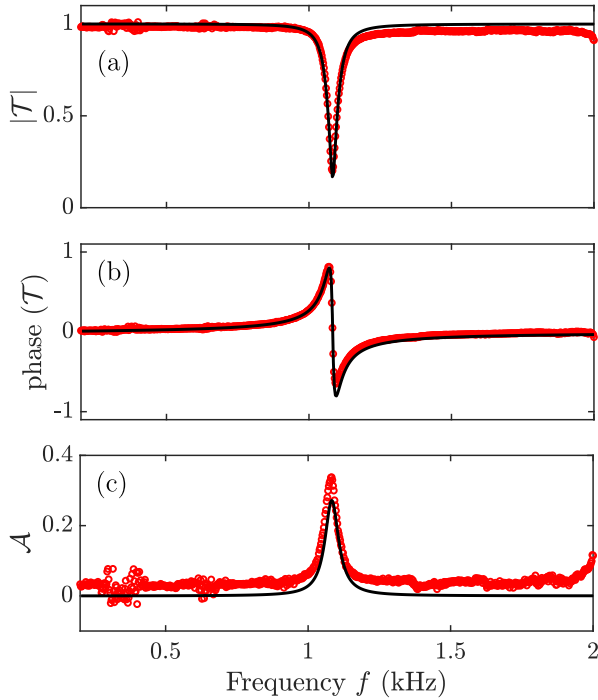


FIG. 2. Example of wave transmission (a) phase (b) and absorption (c) for the elasto-bubble shown in Fig. 1. Red circles: measurements; solid black curves: model prediction with rheology model inclusion¹³. No adjustable parameter used.

ing Eq. (1) into (7) yields

$$\mathcal{T} = 1 + \frac{iKR^*}{\left(\frac{\omega_0}{\omega}\right)^2 - 1 + \frac{2R^*}{R_t} - i(\delta + KR^*)}. \quad (8)$$

This equation predicts a minimum of transmission for $\omega = \omega_0(1 - 2R^*/R_t)^{-1/2}$, *i.e.* slightly above the resonance frequency, due to the coupling between the elasto-bubble and its images. However, the deviation is expected to be low, because the effective acoustic radius of the elasto-bubble is quite small. For elasto-bubble No.2, $R^* \simeq 1.1$ mm, leading to $(1 - 2R^*/R_t)^{-1/2} \simeq 1.02$. The shear modulus of the shell can also bring deviation to simple expression (5). For Ecoflex 00-30, rheological measurements can be found in the literature:¹³ $\mu = \mu_0(1 - (i\omega\tau)^n)$, with $\mu_0 = 26$ kPa, $\tau = 0.26$ ms and $n = 0.33$. With this rheological law, the shear modulus at 1 kHz is of the order of 52 kPa, leading to $12\mu'h/R \simeq 13$ kPa for elasto-bubble No.2, which is indeed small compared to $3\kappa P_0 \simeq 420$ kPa. The approximate resonance frequency (5) is thus expected to give a good prediction of the frequency at which the transmission goes through a minimum. Fig. 3 shows that this is reasonably verified for all the elasto-bubbles we tested.

The position of the minimum of transmission depends only weakly on the rheology of the elastomer, whereas its shape is more sensitive. Indeed, according to Eq. (8) the minimum transmission is given by $\delta/(\delta + KR^*)$, which depends on the viscosity of the shell. As shown in Fig. 2, a very good agreement with the theoretical prediction is found for the complex

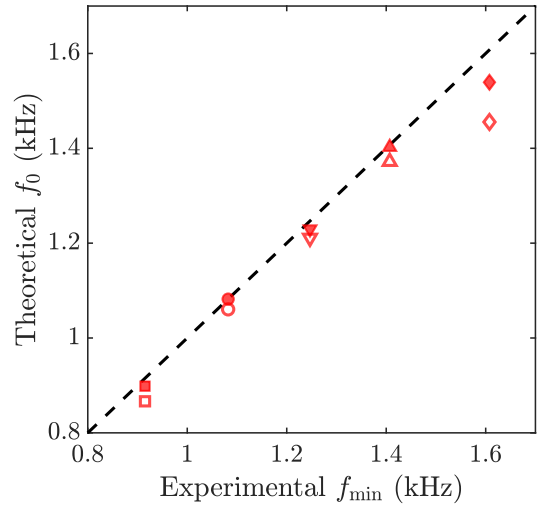


FIG. 3. Theoretical versus experimental frequency f_{\min} for minimum transmission. Hollow symbols correspond to the rheology-free theoretical resonance frequency given by Eq. (5). Solid symbols show the minimum predicted by Eq. (8), which includes the rheology and the coupling effects. Black dashed line: identity line.

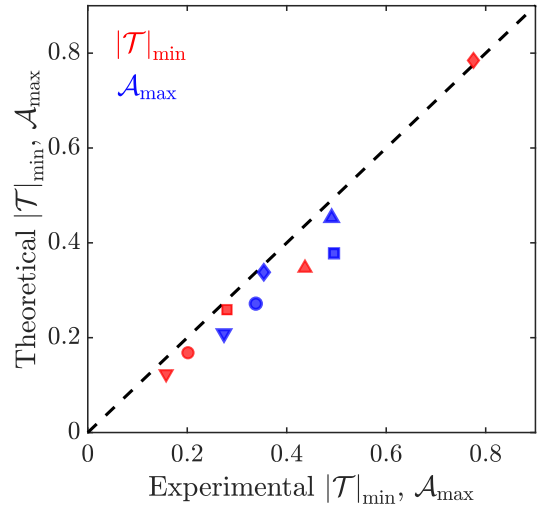


FIG. 4. Red symbols: predicted minimum transmission as a function of the measured minimum transmission $|\mathcal{T}|_{\min}$. Blue symbols: predicted maximum of absorption as a function of the measured peak of absorption \mathcal{A}_{\max} . Black dashed line: identity line.

transmission when considering the rheological law of the literature for the elastomer.

For the absorption (Fig. 2c), the model prediction underestimates the experimental values by a nearly constant offset of about 0.03. It presumably comes from additional losses that are not related to the elasto-bubble, as a comparable level of absorption is measured in the empty tube.

A comparison between the experimental and theoretical minimum of transmission and maximum of absorption is provided in Fig. 4, for the 5 elasto-bubbles of Table I. The agreement is reasonable, demonstrating that the model is efficient in predicting the acoustical response of the elasto-bubbles.

In summary, we showed in this work that these tailored air-filled elasto-bubbles act as efficient subwavelength acoustic resonators with $\lambda \sim 15R$ at resonance. They exhibit a strong transmission dip accompanied by a sharp phase variations and significant absorption, all well described within the formalism of a layered bubble¹ which demonstrate that their acoustic response is fully understood. Moreover, their resonance frequency can be readily tuned by adjusting the radius and shell thickness. In our experiments, this tunability allows us to span a broad frequency range from 800 Hz to 1455 Hz, making these structures promising candidates for acoustic filtering and absorption applications.

ACKNOWLEDGMENTS

DATA AVAILABILITY STATEMENT

All data supporting the findings of this study are available within the manuscript. Additional raw datasets, analysis scripts used to extract wave transmission, phase and absorption are available from the corresponding author upon request.

¹V. Alekseev and S. Rybak, "Gas bubble oscillations in elastic media," *Acoustical Physics* **45**, 535–540 (1999).

²D. R. Smith, J. B. Pendry, and M. C. Wiltshire, "Metamaterials and negative refractive index," *science* **305**, 788–792 (2004).

³J. B. Pendry, A. J. Holden, D. J. Robbins, and W. J. Stewart, "Magnetism from conductors and enhanced nonlinear phenomena," *IEEE transactions on microwave theory and techniques* **47**, 2075–2084 (1999).

⁴G. Ma and P. Sheng, "Acoustic metamaterials: From local resonances to broad horizons," *Science advances* **2**, e1501595 (2016).

⁵N. Fang, D. Xi, J. Xu, M. Ambati, W. Srituravanich, C. Sun, and X. Zhang, "Ultrasonic metamaterials with negative modulus," *Nature materials* **5**, 452–456 (2006).

⁶S. H. Lee, C. M. Park, Y. M. Seo, Z. G. Wang, and C. K. Kim, "Composite acoustic medium with simultaneously negative density and modulus," *Physical review letters* **104**, 054301 (2010).

⁷V. Leroy, A. Strybulevych, M. Lanoy, F. Lemoult, A. Tourin, and J. H. Page, "Superabsorption of acoustic waves with bubble metascreens," *Physical Review B* **91**, 020301 (2015).

⁸M. Minnaert, "Xvi. on musical air-bubbles and the sounds of running water," *The London, Edinburgh, and Dublin Philosophical Magazine and Journal of Science* **16**, 235–248 (1933).

⁹A. Eddi, S. Perrard, and J. Zhang, "Tunable thin elasto-drops," *Soft Matter* (2026).

¹⁰B. Song and J. Bolton, "A transfer-matrix approach for estimating the characteristic impedance and wave numbers of limp and rigid porous materials," *Journal of Acoustical Society of America* **107**, 1131–1152 (1999).

¹¹J. Goldowsky and H. F. Knapp, "Gas penetration through pneumatically driven pdms micro valves," *RSC advances* **3**, 17968–17976 (2013).

¹²H.-X. Rao, F.-N. Liu, and Z.-Y. Zhang, "Preparation and oxygen/nitrogen permeability of pdms crosslinked membrane and pdms/tetraethoxysilicone hybrid membrane," *Journal of Membrane Science* **303**, 132–139 (2007).

¹³A. Delory, F. Lemoult, M. Lanoy, A. Eddi, and C. Prada, "Soft elastomers: A playground for guided waves," *The Journal of the Acoustical Society of America* **151**, 3343–3358 (2022).

¹⁴V. Leroy, A. Strybulevych, M. Scanlon, and J. H. Page, "Transmission of ultrasound through a single layer of bubbles," *The European Physical Journal E* **29**, 123–130 (2009).

¹⁵A. Skvortsov, I. MacGillivray, G. S. Sharma, and N. Kessissoglou, "Sound scattering by a lattice of resonant inclusions in a soft medium," *Physical Review E* **99**, 063006 (2019).